AGU ADVANCING EARTH AND SPACE SCIENCE

Geophysical Research Letters

RESEARCH LETTER
10.1029/2022GL100696

Synoptic Variability in Satellite Altimeter-Derived Radar Freeboard of Arctic Sea Ice

Carmen Nab[1,2], Robbie Mallett[1], William Gregory[1,3], Jack Landy[4], Isobel Lawrence[5,6], Rosemary Willatt[1], Julienne Stroeve[1,7,8], and Michel Tsamados[1]

[1]Centre for Polar Observation and Modelling, University College London, London, UK, [2]Ocean Forecasting Research & Development, Met Office, Exeter, UK, [3]Atmospheric and Oceanic Sciences Program, Princeton University, Princeton, NJ, USA, [4]Department of Physics and Technology, UiT The Arctic University of Norway, Tromsø, Norway, [5]Centre for Polar Observation and Modelling, University of Leeds, Leeds, UK, [6]ESRIN, European Space Agency, Frascati, Italy, [7]Centre for Earth Observation Science, University of Manitoba, Winnipeg, MB, Canada, [8]National Snow and Ice Data Center, University of Colorado Boulder, Boulder, CO, USA

Abstract Satellite observations of sea ice freeboard are integral to the estimation of sea ice thickness. It is commonly assumed that radar pulses from satellite-mounted Ku-band altimeters penetrate through the snow and reflect from the snow-ice interface. We would therefore expect a negative correlation between snow accumulation and radar freeboard measurements, as increased snow loading weighs the ice floe down. In this study we produce daily resolution radar freeboard products from the CryoSat-2 and Sentinel-3 altimeters via a recently developed optimal interpolation scheme. We find statistically significant ($p < 0.05$) positive correlations between radar freeboard anomalies and modeled snow accumulation. This suggests that, in the period after snowfall, radar pulses are not scattering from the snow-ice interface as commonly assumed. Our results offer satellite-based evidence of winter Ku-band radar scattering above the snow-ice interface, violating a key assumption in sea ice thickness retrievals.

Plain Language Summary Arctic sea ice thickness is often estimated using radar pulses from satellite-mounted Ku-band altimeters, which retrieve the *radar freeboard*. This is a proxy for the height of the ice surface above the waterline. Ku-band radar pulses are widely assumed to penetrate through the overlying snowpack and reflect from the top of the sea ice. This means that increased snow loading on a sea ice floe is expected to reduce its radar freeboard, as the snow weighs the sea ice down. We produce daily resolution pan-Arctic radar freeboard data sets from CryoSat-2 and Sentinel-3 retrievals. Using these new products, we find that an increased snow load often increases the radar freeboard, suggesting that the radar pulses are not reflecting off the ice surface. This could explain why satellite-based sea ice thickness estimates don't always match in situ observations.

Key Points:

- We reveal synoptic-scale positive correlations between snow accumulation and Ku-band radar freeboard change
- These correlations indicate that the conventional assumption of full radar-wave penetration of the snowpack does not always hold true
- This sensitivity in freeboard estimates to snow accumulation introduces synoptic variability into satellite estimates of sea ice thickness

Supporting Information:

Supporting Information may be found in the online version of this article.

Correspondence to:

C. Nab,
carmen.nab.18@ucl.ac.uk

Citation:

Nab, C., Mallett, R., Gregory, W., Landy, J., Lawrence, I., Willatt, R., et al. (2023). Synoptic variability in satellite altimeter-derived radar freeboard of Arctic sea ice. *Geophysical Research Letters*, *50*, e2022GL100696. https://doi.org/10.1029/2022GL100696

Received 20 AUG 2022
Accepted 3 JAN 2023

Author Contributions:

Conceptualization: Robbie Mallett
Data curation: Carmen Nab, Jack Landy
Formal analysis: Carmen Nab, Robbie Mallett
Investigation: Carmen Nab
Methodology: William Gregory, Michel Tsamados
Supervision: Michel Tsamados
Writing – original draft: Carmen Nab
Writing – review & editing: Carmen Nab, Robbie Mallett, William Gregory, Jack Landy, Isobel Lawrence, Rosemary Willatt, Julienne Stroeve, Michel Tsamados

1. Introduction

The Arctic's sea ice cover is retreating as the region continues to warm at nearly four times the global average rate (Rantanen et al., 2022). Alongside a decrease in extent and age (Stroeve & Notz, 2018), the sea ice is thinning (Kwok, 2018; Mallett et al., 2021) and snow depth is declining (Stroeve et al., 2020; Webster et al., 2014). A thinning ice pack affects the thermodynamic processes that govern seasonal ice melt and growth, as well as the dynamic processes that control ice mobility (e.g., Rampal et al., 2009). Assimilation of accurate sea ice thickness and snow depth data into models offers an opportunity to improve the prediction of future sea ice state (e.g., Holland et al., 2021; Mignac et al., 2022). Despite the importance of sea ice thickness, the most accurate estimates come from highly localized in situ observations from autonomous ice-buoys or upward-looking sonar instruments. While airborne- or submarine-based campaigns offer greater spatial coverage, they too remain temporally and spatially constrained. Satellite-mounted laser and radar altimeters offer a potential solution by providing year-round, pan-Arctic monitoring.

Several studies have demonstrated an approach to convert Ku-band satellite radar altimeter freeboards from CryoSat-2 (CS2) and Sentinel-3 (S3) to sea ice thickness (Lawrence et al., 2019; Laxon et al., 2013). Sea ice freeboard, the height of the snow-ice interface relative to the surrounding ocean surface, is estimated from the return-time of a radar pulse. Thickness can be derived from the freeboard by applying the assumption of hydrostatic equilibrium together with assumptions concerning the snow, ice and water densities and the snow depth.

All current retrieval techniques operate on the assumption that Ku-band radar waves travel through the overlying snow and return to the detector from the snow-ice interface. However, in its latest assessment report, the IPCC attributed a low confidence in sea ice thickness changes over the satellite period to "snow-induced uncertainties in the retrieval algorithms" (Fox-Kemper et al., 2021, p. 1251).

Increasing snow mass depresses the sea ice into the ocean, theoretically reducing the freeboard. If the assumption of full snowpack penetration were true, we would thus expect a consistent, short-term negative correlation between snow accumulation and freeboard. In addition, deeper snow increases the radar-pulse round-trip time because radar wave propagation is slower in snow than in air (e.g., Tiuri et al., 1984). Therefore, the difference in radar range to a theoretical sea ice surface and the waterline is smaller than the sea ice freeboard itself. This is corrected for in all sea ice thickness retrieval algorithms, though doing so requires knowledge of the overlying snow cover. In this paper we analyze the uncorrected differences, referred to as *radar freeboards*.

If radar waves fully penetrate the snowpack as conventionally assumed, for every centimeter of snow depth accumulation, we would expect an instantaneous reduction in the corresponding radar freeboard of 0.54 cm (see Text S1 in Supporting Information S1) taking into consideration the combined effect of snow weight and radar propagation delay in a ratio of approximately 20:17 (From Equation S9 of Mallett et al., 2021). Were this assumption entirely incorrect, and all radar power were scattered from the air-snow interface rather than the snow-ice interface, we would expect a positive correlation between snow accumulation and radar freeboard. This is the case for ICESat-2 laser freeboard data (Figure S1 in Supporting Information S1). For instance, for snow with a density of 300 kgm^{-3}, accumulation of 1 cm of snow depth generates an expected rise in the ranging surface of 0.71 cm (assuming no compaction due to the weight of snow; see Text S1 in Supporting Information S1 for derivation).

Another factor affecting radar altimetry-derived estimates of sea ice freeboard is the choice of *retracking algorithm* applied to the returned radar waveforms (Landy et al., 2020; Ricker et al., 2014). Raw range measurements between the altimeter and sea ice must be "retracked" to accurately identify the mean snow-ice interface. This is represented by one point on the waveform's leading edge (Quartly et al., 2019), though in reality the radar pulse scatters from multiple heights within the altimeter's footprint. A radar return that is problematically retracked to a height other than the snow-ice interface may thus not necessarily be physically coming from that height. Rather, due to the low range-resolution of the instrument, the radar is receiving power from multiple heights and convolving the signals, resulting in the waveform being retracked to an average height between them. Thus, increased scattering at the snow-air interface may shift the retracking point upwards and decreased scattering would move the retracking point downwards.

In this study we investigate the relationship between snow accumulation and radar freeboard measurements from Ku-band satellite altimeters. In particular, we test whether the mean backscattering height is depressed by an appropriate amount in response to snow accumulation. Where the retrieved freeboard is not depressed by the expected amount, we infer that radar power is not being backscattered from the base of the snowpack. We then test empirical and physical retracking algorithms, assessing which presents the most realistic freeboard depression in response to snow accumulation. Finally, we investigate whether a previously identified relationship between radar freeboard measurements and snowfall (Gregory et al., 2021; Lawrence, 2019) could be explained by meteorological conditions accompanying snowfall.

Ricker et al. (2015) previously characterized a sensitivity of CS2 radar freeboard measurements to snow accumulation using in situ data from buoys. Their study was conducted over the 2012–2014 winter season and compared radar freeboard data (processed using several fixed-threshold retrackers). We build on this work by conducting a pan-Arctic, 10-year analysis using both CS2 and S3 radar freeboard estimates, processed using both a fixed-threshold retracker and a physical retracker.

2. Data and Methods

2.1. Interpolation of Satellite Products

We created two CS2 data sets for each winter season (1 October–30 April) from 2010 to 2020, using two different retrackers:

CS2_CPOM: CS2 radar freeboard data, retracked using the Centre for Polar Observation and Modelling (CPOM) retracker (e.g., Tilling et al., 2018). This is a threshold retracker that determines the retracking point by applying a fixed percentage threshold (70%) to the waveform's first-maximum power return.

CS2_LARM: CS2 radar freeboard data, retracked using the Lognormal Altimeter Retracker Model (LARM) retracker (Landy et al., 2020). This is a physical retracker that varies the percentage threshold according to the sea ice's large-scale roughness.

We then created combined CS2, S3A and S3B (further referred to as CS2S3) radar freeboard data sets as per the methods outlined in Lawrence et al. (2019). This generated a data set with increased track density, reducing our reliance on the interpolation scheme. We produced two data sets for the 2019–2020 winter season:

CS2S3_CPOM: Combined CS2S3 product, retracked using the CPOM retracker. A 1 cm bias correction was applied to S3 to align it with CS2, as per Lawrence et al. (2019).

CS2S3_LARM: Combined CS2S3 product, retracked using the LARM retracker. No bias correction was applied, as no significant median difference was found between the CS2 and S3 data sets over the winter months.

Each of these four data sets was created by binning along-track radar freeboard data onto the 25 km EASE 2.0 grid (Brodzik et al., 2012), with only grid cells containing a sea ice concentration value $\geq$15% selected using the daily sea ice concentration distributions provided by the National Snow and Ice Data Center (NSIDC; Fetterer et al., 2017). Next, we produced four daily resolution pan-Arctic data sets using the along-track data sets listed above from a 9-day moving window ($t \pm 4$ days). We did this using an optimal interpolation scheme following the methods of Gregory et al. (2021), with a fixed hyperparameter climatology S2). The method, Gaussian process regression, is a Bayesian inference technique which updates prior probabilities to learn functional mappings between pairs of observation points in time and space. We provide a full description of this method in Supporting Information S1 (Text S2).

2.2. Snow and Reanalysis Data

To determine the influence of snow accumulation and meteorological variables on radar freeboard retrievals, we used independent snow and weather data. These were regridded onto the same 25 km grid as the freeboard data and are as follows:

Snow depth: Daily estimates from SnowModel-LG (SM-LG; Liston et al., 2020, 2021), a snow evolution model forced with ERA5 weather reanalysis data, that provides daily, pan-Arctic snow property distributions for snow on sea ice. No snow depth data is available for the Canadian Archipelago, so this region was excluded from the analysis. Stroeve et al. (2020) found that SM-LG estimates fall within the range of in situ snow depths taken during the Surface Heat Budget of the Arctic Ocean (SHEBA) and Operation IceBridge campaigns and correlate well with snow buoy measurements taken by the Alfred Wegener Institute (Nicolaus et al., 2021).

Snowfall: Hourly snowfall data from ERA5 (Hersbach et al., 2018), totaled into daily distributions.

Air temperature: Hourly 2 m air temperature data from ERA5 (Hersbach et al., 2018), averaged onto daily distributions.

Wind speed: Hourly u- and v-components from ERA5 (Hersbach et al., 2018), averaged daily and then used to calculate wind speed.

The ERA5 integrated forecast system continuously assimilates satellite radiances over sea ice to model rain and snowfall in the Arctic (Baordo & Geer, 2016). Compared to in situ data from the Multidisciplinary drifting Observatory for the Study of Arctic Climate (MOSAiC) expedition, Wagner et al. (2022) found that ERA5's snowfall magnitudes perform well, with an average overestimation tendency of 3.33 mm when accounting for snowdrift time periods.

2.3. Correlation Analysis

The interpolated radar freeboard data were compared to pan-Arctic daily snow depth, air temperature and wind speed distributions by producing a daily mean and a 31-day running mean of each data set for each grid cell. Then, the difference between the 31-day running mean and the daily mean was taken for each data set to calculate daily anomalies. Next, a 9-day running mean of these anomalies was taken for each data set (further referred to as *smoothed anomalies*) such that an accurate correlation could be determined at synoptic timescales. The limited effect of this smoothing can be seen in Supporting Information S1 (Figure S3). We then calculated the linear correlation coefficient between smoothed anomalies of radar freeboard and snow depth, to determine the sensitivity of Ku-band radar freeboard estimates to snow accumulation on a 9-day timescale. In this analysis, we assume

that the sea ice thickness does not increase anomalously quickly or slowly in a grid cell on the timescale of snow accumulation.

We used the slope of the linear regression between smoothed anomalies of radar freeboard and snow depth to calculate the fractional depth of the snowpack where the retracker detects the radar penetration (α), following Kwok and Cunningham (2015). We calculated α by normalizing the observed ratio of radar freeboard change to snow accumulation (the slope of the linear regression). To set the limits of this normalization procedure, we calculated the expected ratio for full radar penetration of the snowpack (−0.54 m/m, $\alpha = 1$) and for no penetration of the snowpack (0.71 m/m, $\alpha = 0$). We present a derivation of our normalization limits in Supporting Information S1 (Text S1).

We then carried out a partial correlation analysis, to determine whether variation in radar freeboard estimates on synoptic scales is controlled predominantly by snow depth, wind speed, air temperature or a combination of the three. This returns the linear correlation coefficient between one meteorological variable and radar freeboard estimates, while controlling for the influence of the remaining meteorological variables. To do this we defined the partial correlation between variables X and Y, given a set of controlling variables (Z), as the correlation between the residuals of X and Y resulting from the linear regression of X with Z and of Y with Z, respectively (as per p. 178 of Chandler & Scott, 2011).

The sea ice regions defined by the NSIDC (Figure S4 in Supporting Information S1) were used to determine whether a sensitivity in radar freeboard estimate to snow accumulation and meteorological conditions varies by geographical location. Next, the Aaboe (2018) daily sea ice type product was used to compare trends over first-year ice (FYI) and multi-year ice (MYI), with these categories defined as the grid cells classed as FYI/MYI for at least 90% of days in the full 2010–2020 winter season period.

Uncertainty estimates are not produced by SM-LG and are not well-defined for the ERA5 reanalysis product, existing only in the form of ensemble-spreads which do not capture model bias. Furthermore, any uncertainty estimates for radar freeboard values must inherently be linked to an assumption about the *true* mean scattering height—the focus of this paper. Determining the magnitude and propagation of uncertainties in our correlation analysis therefore remains the subject of future work.

3. Results

3.1. Sensitivity of Radar Freeboard Measurements to Snow Accumulation

We now illustrate the sensitivity of radar freeboard values to snow accumulation using the 10-year CS2_CPOM data set. Over the full 10-year period of data availability, we find a negative correlation between radar freeboard estimates and snow accumulation in areas dominated by MYI such as the Central Arctic (Figure 1a). Of the grid cells with statistically significant correlations in the Central Arctic, 50% of the correlations are positive. The mean ratio between radar freeboard change and snow depth change in these grid cells is 0.07 m/m (compared to the −0.54 m/m expected; Figure S5a in Supporting Information S1). The remaining statistically significant negatively correlated grid cells have a mean ratio of −0.07 m/m. In the marginal seas, 66% of the statistically significant grid cells showed a positive correlation, with a mean ratio of 0.20 m/m. In comparison, the mean ratio of the negatively correlated statistically significant grid cells in the marginal seas is −0.26 m/m. We find that these spatial patterns in correlation coefficients are consistent when compared to those found using radar freeboard data produced using a simple distance/time-weighted interpolation method (Figure S6 in Supporting Information S1).

In our regional analysis, we find statistically significant positive correlations ($p < 0.05$) between smoothed anomalies of radar freeboard and snow depth for the majority of winter seasons in the 2010–2020 period in the Greenland, Laptev, East Siberian, and Chukchi regions (Figure 1b). We find an inter-annual variation in the magnitude and sign of these correlations (Figure S7 in Supporting Information S1). For example, in Baffin Bay, we find a decrease in radar freeboard of 0.36 cm for every 1 cm of snow accumulation over the 2011–2012 winter season compared to an increase in radar freeboard of 0.61 cm for every 1 cm of snow accumulation over the following winter season (Figure S5b in Supporting Information S1).

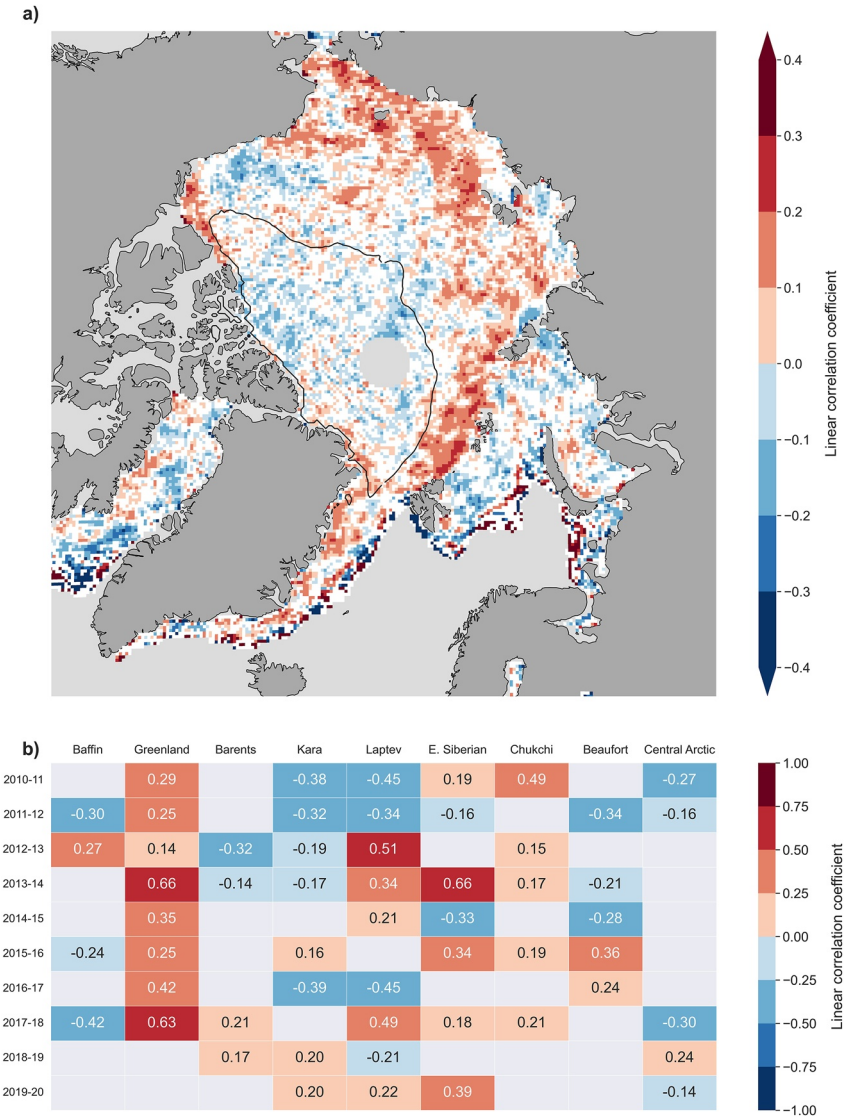

Figure 1. (a) Grid cell-by-grid cell correlation between smoothed anomalies of CS2_CPOM interpolated freeboard and SnowModel-LG (SM-LG) snow depth over 10 winter seasons (1 October–30 April), from 2010 to 2020. Cells where $p > 0.05$ are shown in white, to show only statistically significant results. Black contour line indicates the region where sea ice is multi-year ice for at least 50% of the full 2010–2020 winter season period. (b) Regional correlation between smoothed anomalies of CS2_CPOM interpolated freeboard and SM-LG snow depth per winter season (1 October–30 April), with cells where $p > 0.05$ grayed out to show only statistically significant results. Only days where both freeboard and snow depth data are available are included for each grid cell for both subplots.

For the positively correlated grid cells, the slope of the linear regression between radar freeboard estimate and snow depth peaks in the Barents region, where a radar freeboard increase of 0.70 cm is found for every 1 cm of snow depth increase over the 2018–2019 winter season (Figure S5b in Supporting Information S1). Using this slope, we calculate $0.4 \leq \alpha \leq 0.8$, with the highest values found in October. We find a decrease in α between October–December, with the values staying relatively stable between December–March (Figure 2). We find an increase in the prevalence of positive correlations over time, with 72% of the statistically significant regional seasonal correlations found to be positive over the 2015–2020 period, compared to 47% over the 2010–2015 period (Figure 1b). These spatial patterns and correlation magnitudes were found to be consistent when comparing the CS2_CPOM data set to the higher temporal resolution CS2S3_CPOM data set over the 2019–2020 winter season (Figure S8 in Supporting Information S1).

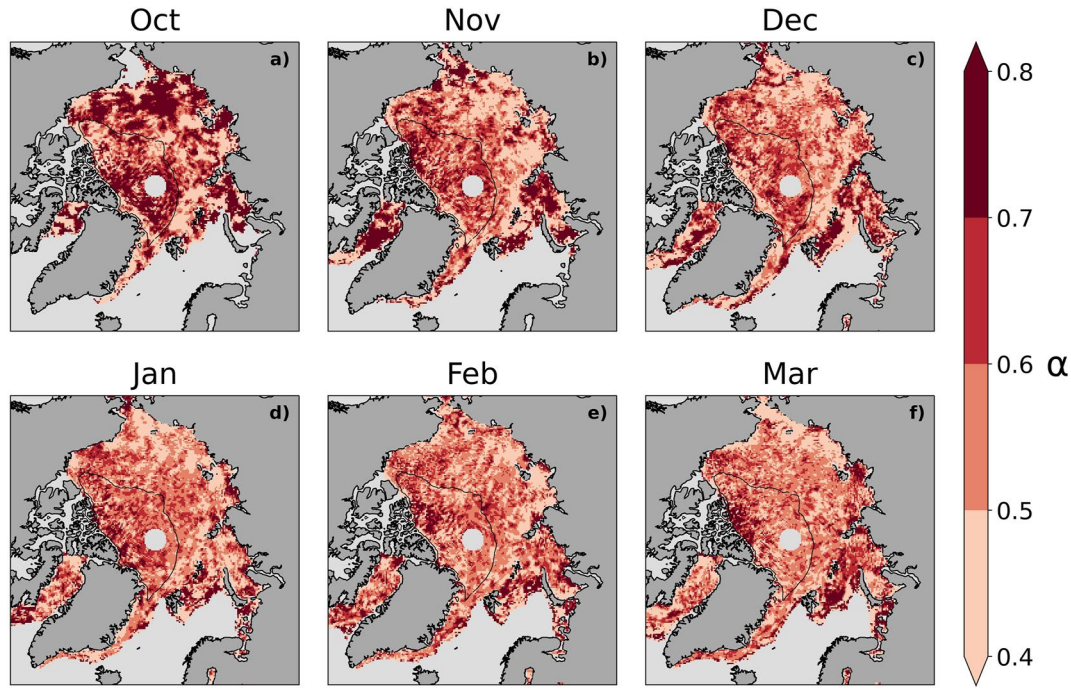

Figure 2. Monthly grid cell-by-grid cell α for the CS2_CPOM interpolated freeboard over 10 winter seasons, from 2010 to 2020 for October to March (a–f). Black contour line indicates the region where sea ice is multi-year ice for at least 50% of the full 2010–2020 winter season period.

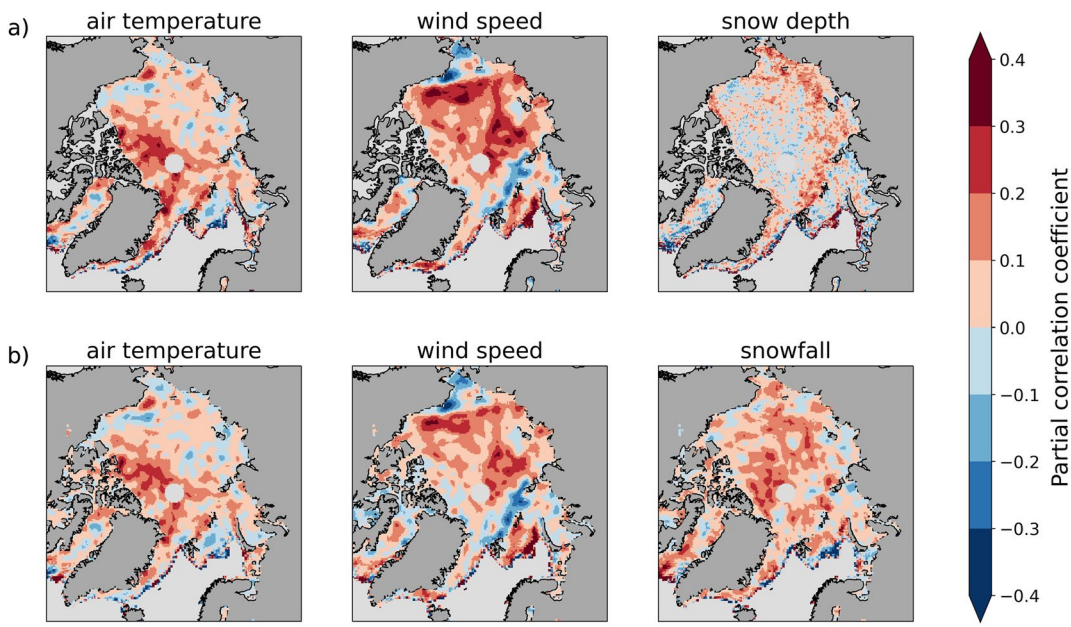

Figure 3. Partial correlation coefficient between smoothed anomalies of CS2_CPOM interpolated freeboard estimate and smoothed anomalies of (a) air temperature, wind speed and snow depth (b) air temperature, wind speed and snowfall for the full 2010–2020 winter season period. This shows the correlation coefficient between one meteorological variable and radar freeboard estimates, while controlling for influence of the remaining meteorological variables. All cells are shown regardless of statistical significance.

3.2. Sensitivity of Radar Freeboard Values to Air Temperature and Wind Speed

To determine whether a previously determined relationship between snowfall and radar freeboard estimate (Gregory et al., 2021; Lawrence, 2019) can be explained by the meteorological conditions that tend to accompany snowfall, we investigate the impact of air temperature and wind speed on radar freeboard returns. Our partial correlation results (Figure 3) show broadly different behaviors in the Central Arctic by comparison to the marginal seas. This is clearly the case for wind speed, where correlations are more positive in the Central Arctic and more negative in the marginal seas. The case is more nuanced for the air temperature results, where strong negative correlations exist in the Chukchi Sea and North of Svalbard and Franz Josef Land. Elsewhere the pattern is similar to the wind speed plots: more negative results in the Central Arctic compared to the Beaufort, East Siberian and Laptev marginal seas. Turning to the snow anomalies, it is striking that depth anomalies in the Central Arctic are negatively correlated with radar freeboard anomalies, whereas snowfall anomalies are positively correlated. The spatial patterning of negative correlations in Figure 3a indicates that this may relate to the ice type, with negative correlations dominating in the Arctic Ocean's MYI section. We discuss potential causes of this in Section 4.2.

3.3. Relative Sensitivity of Empirical and Physical Retrackers to Snow Accumulation

The sensitivity of radar freeboard estimates to snow accumulation is in part determined by the method used to retrack the radar waveforms. Comparing correlations between snow accumulation and the CS2_CPOM freeboard data to those for the CS2_LARM freeboard data reveals an overall consistency in correlation coefficients and spatial patterns, though the prevalence of positive correlation coefficients was found to be higher when using the LARM-retracked freeboard data (Figure S9 in Supporting Information S1). In our previous regional correlation analysis between CS2_CPOM radar freeboard data and snow depth over each winter season from 2010 to 2020, 58% of statistically significant correlations were found to be positive (Figure 1), compared to 74% for CS2_LARM (Figure S9a in Supporting Information S1). For both retrackers, no negative correlations were found in the Greenland Sea region. Of the winter seasons that show statistically significant correlations, FYI-dominated grid cells exhibited an overall positive correlation in 50% of seasons for the CS2_CPOM data, compared to 100% for CS2_LARM. MYI-dominated grid cells exhibited positive correlations for 63% and 57% of winter seasons for the CPOM and LARM retrackers respectively (Figure S10 in Supporting Information S1).

Both the merged data sets (CS2S3_CPOM & CS2S3_LARM) show positive correlation coefficients to snow depth in the Baffin, Laptev and E. Siberian regions over the 2019–2020 winter season (Figure S9 in Supporting Information S1). The CS2S3_LARM data shows positive correlations in 16% more grid cells than the CS2S3_CPOM data. As a whole, FYI-dominated grid cells showed a positive correlation and MYI-dominated grid cells a negative correlation for both the CS2S3_CPOM and CS2S3_LARM freeboards (Figure S10 in Supporting Information S1).

4. Discussion and Conclusions

4.1. Sensitivity of Freeboard Retrievals to Weather

We suggest that the positive correlations between radar freeboard measurements and air temperature result from a modification of the snow surface, changing the backscattering power of the snow-air interface. One potential driver of this could be increases in the liquid water content of the saline snow, which may drive an increase in the dielectric contrast at the air-snow interface (A. Fung & Chen, 2004). However, the positive correlations between air temperature and radar freeboard anomalies appear across most of the Arctic Ocean, including areas dominated by MYI where snow is generally not saline (Figure S11 in Supporting Information S1). Another possible driver is thermodynamic modification of the snow microstructure; warmer air temperatures accelerate temperature gradient metamorphism (e.g., Marbouty, 1980), which alters the physical structure and microwave scattering properties of snow (Mätzler, 1998). We find that in larger regions, such as the Central Arctic, both positive and negative temperature anomalies are present in the same region on the same day, such that they largely compensate for each other within large-scale averages: This can produce correlation coefficients of unrealistically large magnitudes that do not reflect synoptic-scale variability. Our general findings regarding air temperature are in line with those of Willatt et al. (2011), who concluded that airborne Ku-band radar waves "penetrat[ed] further into the snow cover at low temperatures".

We suggest several potential mechanisms for the apparent control of wind on radar freeboard measurements. The snow surface roughness at small length scales (that of the radar wavelength, ∼1 cm in this case) is modified by wind, as particles break down and saltate (Gromke et al., 2011; Löwe et al., 2007). Small changes in the wavelength-scale roughness may drive significant changes in backscatter and transmission at the snow-air interface (A. K. Fung, 2015), thus changing the retracked height of the waveform (see Text S3; Figure S12 in Supporting Information S1). We also suggest that higher winds may rearrange larger-scale snow topography, such as dunes and sastrugi. The height distribution of the snow surface likely influences the radar waveform whenever any power returns from the snow-air interface (Landy et al., 2019). If the snow is topographically flattened or roughened, the appropriate method of retracking should likely change (Fetterer et al., 1992; Nandan et al., 2022; Tonboe et al., 2006). Finally, the density-contrast at the snow-air interface may be enhanced by wind through the process of *wind packing* (Sturm & Massom, 2009). During this process, the density of the snow surface increases significantly, potentially providing a more scattering surface. For example, an increase in snow density from 250 to 350 kgm^{-3} at a rough snow surface can drive a 171% increase in the modeled surface backscattering (see Text S3; Figure S13 in Supporting Information S1).

While we did find correlations between radar freeboard returns and meteorological conditions, these cannot be used to fully explain the sensitivity of radar freeboard estimates to snow accumulation. We argue that the snow properties that vary as a result of fresh snow accumulation, temperature and wind, such as brine volume fraction, grain size and roughness together determine the variability in the radar freeboard returns (as in Landy et al. (2020); Nandan et al. (2017, 2020)). With an increase in Arctic precipitation, temperature and storminess already observed as a result of climate change (Crawford et al., 2022; Semenov et al., 2019; Sepp & Jaagus, 2011), we caution that the assumption of full penetration may become increasingly less applicable as the geophysical properties of the snowpack change and the growth season shortens. An increase in the resulting bias in radar freeboard estimates in the future would represent a problem for Ku-band altimeter-derived sea ice thickness and snow depth calculations.

4.2. Sensitivity of Radar Freeboard Measurements to Snow Accumulation

Our results show diverse and non-intuitive radar freeboard responses to snow accumulation over synoptic scales, meaning that short term variations in retrieved freeboard may reflect short-term changes in snow properties rather than variation in the elevation of the snow-ice interface. Satellite altimeter validation experiments are often conducted by comparing satellite retrievals to in situ observations on the day of in situ data collection. The synoptic-scale response of satellite radar freeboard estimates to snow accumulation may explain the sometimes large differences between in situ and satellite-derived sea ice thickness measurements (e.g., Figure 16 of Tilling et al., 2018), as the accuracy of satellite altimeter-derived sea ice thickness on a specific day may not be representative of the accuracy on adjacent days. Additionally, spatial variation in the sensitivity of radar freeboard estimates to snow accumulation means that regional differences in sea ice thickness cannot currently be accurately compared over synoptic length scales. The findings hold true in an analysis of the CS2S3 data sets, showing that the different results between the Central Arctic and the marginal seas cannot be explained by a lower data density over the marginal seas when using only CS2 data.

The positive correlations between snow accumulation and freeboard suggest that backscattered radar power may, in part, be originating above the snow-ice interface (as indicated by Willatt et al., 2011, for airborne radar retrievals). This means that, after retracking, the retrieval responds more like a laser altimeter to snow accumulation than a conventionally understood Ku-band radar altimeter. Unlike these radar altimeters, there is a negative relationship to snow for laser-based sea ice thickness estimates, such that the derived thickness of the underlying sea ice decreases with increased snow depth (Equation 1 of Petty et al., 2020). A radar altimeter behaving in this way would significantly overestimate sea ice thickness. This is particularly the case given that biases in the radar scattering height only ever introduce an overestimating bias on the ice freeboard, which are magnified 10-fold in the conversion to sea ice thickness. However, sea ice thickness retrievals generally have a fairly low aggregated bias when evaluated against in situ sources (Tilling et al., 2018). This indicates the action of other, compensating biases on sea ice thickness that result in retrievals being centered around observed values while having a large spread around those values. The source of these compensating biases may involve the sensitivity of the returned waveform to surface roughness (e.g., Landy et al., 2020) or the large uncertainties in sea ice density (e.g., Jutila et al., 2022).

We would expect the correlation between snow depth and radar freeboard measurements to be negative where $\alpha > 0.55$ and positive where $\alpha < 0.55$ (assuming a snow density of 300 kg/m^3; Lawrence, 2019). This means that for a positive correlation to be found, the mean backscattering height must be located in the top 55% of the snowpack. While this may be the case when there are positive snow anomalies, the average height may drop back toward the snow-ice interface in intervening periods, as the radar freeboard falls when there is anomalously low snow accumulation. This suggests a radar freeboard response specific to recent snowfall, such as density differences between snow layers, a characteristic wavelength-scale roughness, or warming of the snowpack base and snow-ice interface due to thermal insulation.

The LARM-retracked freeboard data showed a higher sensitivity to snow accumulation than the CPOM-retracked data. The LARM retracker sets a variable threshold on the waveform, based on the algorithm's assessment of the topographic roughness within the altimeter footprint. We propose that the higher prevalence of positive correlations to snow depth in the LARM retracker is caused by a change in the radar waveform as a result of new snow accumulation, which reduces the threshold assigned by the algorithm and raises the radar freeboard.

We find positive correlation coefficients between radar freeboard change and snowfall anomalies over both FYI and MYI, consistent with the results found by Gregory et al. (2021). When using snow depth instead of snowfall, we find primarily positive correlation coefficients over FYI and primarily negative correlation coefficients over MYI. We speculate that this behavioral bifurcation for snow depth and not snowfall correlations results from the presence of the multi-year snowpack in September and October: Snow on MYI accumulates and metamorphoses in these warmer, higher-precipitation months, which may drive differences in the subsequent evolution.

4.3. Implications for Dual-Frequency Snow Estimation and the CRISTAL Mission

The proposed CRISTAL mission houses a dual-frequency altimeter operating at both Ku- and Ka-band, aimed at improving sea ice thickness and snow depth retrievals (Kern et al., 2020). It has been argued that Ka-band altimeters such as AltiKa respond to snow accumulation similarly to laser altimeters (e.g., Garnier et al., 2021), in that snow penetration is negligible in both cases. By performing the same analysis on Ka-band retrievals from AltiKa as was performed on the Ku-band altimeters above, we find the Ka-band response to snow accumulation to be somewhere in between the responses of Ku-band and laser retrievals (Figure S14 in Supporting Information S1). Furthermore, AltiKa retrievals appear to be more sensitive to the choice of retracking method (LARM vs. CPOM) than Ku-band retrievals (Figure S15 in Supporting Information S1).

Snow depth has been estimated from coincident Ku- and Ka-band retrievals (e.g., Guerreiro et al., 2016) by calibrating them to align the Ka-band observations with the snow surface and the Ku-band observations with the snow-ice interface (e.g., Lawrence et al., 2018). In this paper we have focused on the response of Ku-band retrievals; our analysis here raises the prospects that the assumption of negligible Ka-band penetration into snow may not always be accurate and that the methods used in this paper could be deployed in future on retrievals from the AltiKa and CRISTAL missions.

Our results show a regionally dependent instantaneous response of Ku-band radar freeboard estimates to snow accumulation with varying sign and magnitude. This means that the mean backscattering height of Ku-band radar waves is not necessarily coincident with the snow-ice interface, and instead responds to properties of the overlying snow. To account for this sensitivity, a sea ice thickness retrieval algorithm would need to incorporate information on snow properties such as depth, roughness and snow water equivalent to gather more information on where the mean backscattering height is at a specific point in time. Thus, the success of the upcoming CRISTAL mission in retrieving the depth of snow on sea ice may require additional processing steps in order to account for the sensitivity of Ku-band radar freeboard estimates to snow accumulation.

Data Availability Statement

All code required to reproduce this analysis can be found at https://doi.org/10.5281/zenodo.7271744 (Nab, 2022a). The daily resolution interpolated freeboard data can be found at https://doi.org/10.5281/zenodo.6401726 (Nab, 2022b). The SM-LG snow depth data can be found at https://doi.org/10.5067/27A0P5M6LZBI (Liston et al., 2021). The ERA5 snowfall, air temperature and wind speed data can be found at https://doi.org/10.24381/cds.adbb2d47 (Hersbach et al., 2018).

Acknowledgments
CN acknowledges support from NERC (NE/S007229/1) and the Met Office (CASE Partnership). RM acknowledges support from NERC (NE/L002485/1). WG acknowledges M^{2}LInES research funding by the generosity of Eric and Wendy Schmidt by recommendation of the Schmidt Futures program. RW acknowledges support from NERC (NE/S002510/1). JL acknowledges support from the CIRFA project through the RCN (RCN237906). JS acknowledges support from the Canada 150 Chair Program and NASA Grants NNX16AJ92G, 80NSSC20K1121, and 19-ICESAT2-19-0088; "Sunlight under sea ice." MT acknowledges support from ESA (ESA/AO/1-9132/17/NL/MP and ESA/AO/1-10061/19/I-EF) and NERC (NE/T000546/1 and NE/X004643/1).

References

Aaboe, S. (2018). Sea ice edge and type daily gridded data from 1979 to present derived from satellite observations. *Copernicus*. https://doi.org/10.24381/CDS.29C46D83

Baordo, F., & Geer, A. J. (2016). Assimilation of SSMIS humidity-sounding channels in all-sky conditions over land using a dynamic emissivity retrieval. *Quarterly Journal of the Royal Meteorological Society*, *142*(700), 2854–2866. https://doi.org/10.1002/qj.2873

Brodzik, M. J., Billingsley, B., Haran, T., Raup, B., & Savoie, M. H. (2012). EASE-grid 2.0: Incremental but significant improvements for Earth-gridded data sets. *ISPRS International Journal of Geo-Information*, *1*(1), 32–45. https://doi.org/10.3390/ijgi1010032

Chandler, R. E., & Scott, E. M. (Eds.). (2011). *Statistical methods for trend detection and analysis in the environmental sciences: Chandler/statistical methods for trend detection and analysis in the environmental sciences*. John Wiley & Sons, Ltd. https://doi.org/10.1002/9781119991571

Crawford, A. D., Lukovich, J. V., McCrystall, M. R., Stroeve, J. C., & Barber, D. G. (2022). Reduced sea ice enhances intensification of winter storms over the Arctic Ocean. *Journal of Climate*, *35*(11), 1–39. https://doi.org/10.1175/JCLI-D-21-0747.1

Fetterer, F. M., Drinkwater, M. R., Jezek, K. C., Laxon, S. W. C., Onstott, R. G., & Ulander, L. M. H. (1992). Sea ice altimetry. In *Geophysical monograph series* (Vol. 68, pp. 111–135). American Geophysical Union. https://doi.org/10.1029/GM068p0111

Fetterer, F. M., Knowles, K., Meier, W., Savoie, M., & Windnagel, A. (2017). *Sea ice index, version 3*. NSIDC. https://doi.org/10.7265/N5K072F8

Fox-Kemper, B., Hewitt, H., Xiao, C., Adalgeirsdóttir, G., Drijfhout, S., Edwards, T., et al. (2021). Ocean, cryosphere and sea level change. In *Climate change 2021: The physical science basis. Contribution of working group I to the sixth assessment report of the intergovernmental panel on climate change* (pp. 1211–1362). https://doi.org/10.1017/9781009157896.011

Fung, A., & Chen, K. (2004). An update on the IEM surface backscattering model. *IEEE Geoscience and Remote Sensing Letters*, *1*(2), 75–77. https://doi.org/10.1109/LGRS.2004.826564

Fung, A. K. (2015). *Backscattering from multiscale rough surfaces with application to wind scatterometry*. Artech House.

Garnier, F., Fleury, S., Garric, G., Bouffard, J., Tsamados, M., Laforge, A., et al. (2021). Advances in altimetric snow depth estimates using bi-frequency SARAL and CryoSat-2 Ka–Ku measurements. *The Cryosphere*, *15*(12), 5483–5512. https://doi.org/10.5194/tc-15-5483-2021

Gregory, W., Lawrence, I. R., & Tsamados, M. (2021). A Bayesian approach towards daily pan-Arctic sea ice freeboard estimates from combined CryoSat-2 and Sentinel-3 satellite observations. *The Cryosphere*, *15*(6), 2857–2871. https://doi.org/10.5194/tc-15-2857-2021

Gromke, C., Manes, C., Walter, B., Lehning, M., & Guala, M. (2011). Aerodynamic roughness length of fresh snow. *Boundary-Layer Meteorology*, *141*(1), 21–34. https://doi.org/10.1007/s10546-011-9623-3

Guerreiro, K., Fleury, S., Zakharova, E., Rémy, F., & Kouraev, A. (2016). Potential for estimation of snow depth on Arctic sea ice from CryoSat-2 and SARAL/AltiKa missions. *Remote Sensing of Environment*, *186*, 339–349. https://doi.org/10.1016/j.rse.2016.07.013

Hersbach, H., Bell, B., Berrisford, P., Biavati, G., Horányi, A., Muñoz Sabater, J., et al. (2018). ERA5 hourly data on single levels from 1979 to present. *Copernicus Climate Change Service (C3S) Climate Data Store (CDS)*. https://doi.org/10.24381/cds.adbb2d47

Holland, M. M., Clemens-Sewall, D., Landrum, L., Light, B., Perovich, D., Polashenski, C., et al. (2021). The influence of snow on sea ice as assessed from simulations of CESM2. *The Cryosphere*, *15*(10), 4981–4998. https://doi.org/10.5194/tc-15-4981-2021

Jutila, A., Hendricks, S., Ricker, R., von Albedyll, L., Krumpen, T., & Haas, C. (2022). Retrieval and parameterisation of sea-ice bulk density from airborne multi-sensor measurements. *The Cryosphere*, *16*(1), 259–275. https://doi.org/10.5194/tc-16-259-2022

Kern, M., Cullen, R., Berruti, B., Bouffard, J., Casal, T., Drinkwater, M. R., et al. (2020). The Copernicus polar ice and snow topography altimeter (CRISTAL) high-priority candidate mission. *The Cryosphere*, *14*(7), 2235–2251. https://doi.org/10.5194/tc-14-2235-2020

Kwok, R. (2018). Arctic sea ice thickness, volume, and multiyear ice coverage: Losses and coupled variability (1958–2018). *Environmental Research Letters*, *13*(10), 105005. https://doi.org/10.1088/1748-9326/aae3ec

Kwok, R., & Cunningham, G. F. (2015). Variability of Arctic sea ice thickness and volume from CryoSat-2. *Philosophical Transactions of the Royal Society A: Mathematical, Physical & Engineering Sciences*, *373*(2045), 20140157. https://doi.org/10.1098/rsta.2014.0157

Landy, J. C., Petty, A. A., Tsamados, M., & Stroeve, J. C. (2020). Sea ice roughness overlooked as a key source of uncertainty in CryoSat-2 ice freeboard retrievals. *Journal of Geophysical Research: Oceans*, *125*(5). https://doi.org/10.1029/2019JC015820

Landy, J. C., Tsamados, M., & Scharien, R. K. (2019). A facet-based numerical model for simulating SAR altimeter echoes from heterogeneous sea ice surfaces. *IEEE Transactions on Geoscience and Remote Sensing*, *57*(7), 4164–4180. https://doi.org/10.1109/TGRS.2018.2889763

Lawrence, I. R. (2019). *Multi-satellite synergies for polar ocean altimetry (PhD)*. University College London.

Lawrence, I. R., Armitage, T. W., Tsamados, M. C., Stroeve, J. C., Dinardo, S., Ridout, A. L., et al. (2019). Extending the Arctic sea ice freeboard and sea level record with the Sentinel-3 radar altimeters. *Advances in Space Research*, *68*(2), 711–723. https://doi.org/10.1016/j.asr.2019.10.011

Lawrence, I. R., Tsamados, M. C., Stroeve, J. C., Armitage, T. W. K., & Ridout, A. L. (2018). Estimating snow depth over Arctic sea ice from calibrated dual-frequency radar freeboards. *The Cryosphere*, *12*(11), 3551–3564. https://doi.org/10.5194/tc-12-3551-2018

Laxon, S. W., Giles, K. A., Ridout, A. L., Wingham, D. J., Willatt, R., Cullen, R., et al. (2013). CryoSat-2 estimates of Arctic sea ice thickness and volume. *Geophysical Research Letters*, *40*(4), 732–737. https://doi.org/10.1002/grl.50193

Liston, G. E., Itkin, P., Stroeve, J., Tschudi, M., Stewart, J. S., Pedersen, S. H., et al. (2020). A Lagrangian snow-evolution system for sea-ice applications (SnowModel-LG): Part I—Model description. *Journal of Geophysical Research: Oceans*, *125*(10), e2019JC015913. https://doi.org/10.1029/2019JC015913

Liston, G. E., Stroeve, J., & Itkin, P. (2021). *Lagrangian snow distributions for sea-ice applications, version 1*. ERA5 Subset. NASA National Snow and Ice Data Center DAAC. https://doi.org/10.5067/27A0P5M6LZBI

Löwe, H., Egli, L., Bartlett, S., Guala, M., & Manes, C. (2007). On the evolution of the snow surface during snowfall. *Geophysical Research Letters*, *34*(21), L21507. https://doi.org/10.1029/2007GL031637

Mallett, R. D. C., Stroeve, J. C., Tsamados, M., Landy, J. C., Willatt, R., Nandan, V., & Liston, G. E. (2021). Faster decline and higher variability in the sea ice thickness of the marginal Arctic seas when accounting for dynamic snow cover. *The Cryosphere*, *15*(5), 2429–2450. https://doi.org/10.5194/tc-15-2429-2021

Marbouty, D. (1980). An experimental study of temperature-gradient metamorphism. *Journal of Glaciology*, *26*(94), 303–312. https://doi.org/10.3189/S0022143000010844

Mätzler, C. (1998). Improved born approximation for scattering of radiation in a granular medium. *Journal of Applied Physics*, *83*(11), 6111–6117. https://doi.org/10.1063/1.367496

Mignac, D., Martin, M., Fiedler, E., Blockley, E., & Fournier, N. (2022). Improving the Met Office's Forecast Ocean Assimilation Model (FOAM) with the assimilation of satellite-derived sea-ice thickness data from CryoSat-2 and SMOS in the Arctic. *Quarterly Journal of the Royal Meteorological Society*, *148*(744), 4252–1167. https://doi.org/10.1002/qj.4252

Nab, C. (2022a). carmennab/ku_snow: v1 (Version v1). *Zenodo*. https://doi.org/10.5281/zenodo.7271745

Nab, C. (2022b). Daily-resolution pan-Arctic Radar and Laser Freeboard. *Zenodo*. https://doi.org/10.5281/zenodo.7327572

Nandan, V., Geldsetzer, T., Yackel, J., Mahmud, M., Scharien, R., Howell, S., et al. (2017). Effect of snow salinity on CryoSat-2 Arctic first-year sea ice freeboard measurements: Sea ice brine-snow effect on CryoSat-2. *Geophysical Research Letters*, *44*(20), 10419–10426. https://doi.org/10.1002/2017GL074506

Nandan, V., Scharien, R. K., Geldsetzer, T., Kwok, R., Yackel, J. J., Mahmud, M. S., et al. (2020). Snow property controls on modeled Ku-band altimeter estimates of first-year sea ice thickness: Case studies from the Canadian and Norwegian Arctic. *IEEE Journal of Selected Topics in Applied Earth Observations and Remote Sensing*, *13*, 1082–1096. https://doi.org/10.1109/JSTARS.2020.2966432

Nandan, V., Willatt, R., Mallett, R., Stroeve, J., Geldsetzer, T., Scharien, R., et al. (2022). Wind transport of snow impacts Ka- and Ku-band radar signatures on Arctic sea ice. *The Cryosphere Discussions*. https://doi.org/10.5194/tc-2022-116

Nicolaus, M., Hoppmann, M., Arndt, S., Hendricks, S., Katlein, C., Nicolaus, A., et al. (2021). Snow depth and air temperature seasonality on sea ice derived from snow buoy measurements. *Frontiers in Marine Science*, *8*, 655446. https://doi.org/10.3389/fmars.2021.655446

Petty, A. A., Kurtz, N. T., Kwok, R., Markus, T., & Neumann, T. A. (2020). Winter Arctic sea ice thickness from ICESat-2 freeboards. *Journal of Geophysical Research: Oceans*, *125*(5). https://doi.org/10.1029/2019JC015764

Quartly, G. D., Rinne, E., Passaro, M., Andersen, O. B., Dinardo, S., Fleury, S., et al. (2019). Retrieving sea level and freeboard in the Arctic: A review of current radar altimetry methodologies and future perspectives. *Remote Sensing*, *11*(7), 881. https://doi.org/10.3390/rs11070881

Rampal, P., Weiss, J., & Marsan, D. (2009). Positive trend in the mean speed and deformation rate of Arctic sea ice, 1979–2007. *Journal of Geophysical Research*, *114*(C5), C05013. https://doi.org/10.1029/2008JC005066

Rantanen, M., Karpechko, A. Y., Lipponen, A., Nordling, K., Hyvärinen, O., Ruosteenoja, K., et al. (2022). The Arctic has warmed nearly four times faster than the globe since 1979. *Communications Earth & Environment*, *3*(1), 168. https://doi.org/10.1038/s43247-022-00498-3

Ricker, R., Hendricks, S., Helm, V., Skourup, H., & Davidson, M. (2014). Sensitivity of CryoSat-2 Arctic sea-ice freeboard and thickness on radar-waveform interpretation. *The Cryosphere*, *8*(4), 1607–1622. https://doi.org/10.5194/tc-8-1607-2014

Ricker, R., Hendricks, S., Perovich, D. K., Helm, V., & Gerdes, R. (2015). Impact of snow accumulation on CryoSat-2 range retrievals over Arctic sea ice: An observational approach with buoy data. *Geophysical Research Letters*, *42*(11), 4447–4455. https://doi.org/10.1002/2015GL064081

Semenov, A., Zhang, X., Rinke, A., Dorn, W., & Dethloff, K. (2019). Arctic intense summer storms and their impacts on sea ice—A regional climate modeling study. *Atmosphere*, *10*(4), 218. https://doi.org/10.3390/atmos10040218

Sepp, M., & Jaagus, J. (2011). Changes in the activity and tracks of Arctic cyclones. *Climatic Change*, *105*(3–4), 577–595. https://doi.org/10.1007/s10584-010-9893-7

Stroeve, J., Liston, G. E., Buzzard, S., Zhou, L., Mallett, R., Barrett, A., et al. (2020). A Lagrangian snow evolution system for sea ice applications (SnowModel-LG): Part II—Analyses. *Journal of Geophysical Research: Oceans*, *125*(10), e2019JC015900. https://doi.org/10.1029/2019JC015900

Stroeve, J., & Notz, D. (2018). Changing state of Arctic sea ice across all seasons. *Environmental Research Letters*, *13*(10), 103001. https://doi.org/10.1088/1748-9326/aade56

Sturm, M., & Massom, R. A. (2009). Snow and sea ice. In *Sea ice* (pp. 153–204). Wiley-Blackwell.

Tilling, R. L., Ridout, A., & Shepherd, A. (2018). Estimating Arctic sea ice thickness and volume using CryoSat-2 radar altimeter data. *Advances in Space Research*, *62*(6), 1203–1225. https://doi.org/10.1016/j.asr.2017.10.051

Tiuri, M., Sihvola, A., Nyfors, E., & Hallikaiken, M. (1984). The complex dielectric constant of snow at microwave frequencies. *IEEE Journal of Oceanic Engineering*, *9*(5), 377–382. https://doi.org/10.1109/JOE.1984.1145645

Tonboe, R., Andersen, S., & Pedersen, L. (2006). Simulation of the Ku-band radar altimeter sea ice effective scattering surface. *IEEE Geoscience and Remote Sensing Letters*, *3*(2), 237–240. https://doi.org/10.1109/LGRS.2005.862276

Wagner, D. N., Shupe, M. D., Cox, C., Persson, O. G., Uttal, T., Frey, M. M., et al. (2022). Snowfall and snow accumulation during the MOSAiC winter and spring seasons. *The Cryosphere*, *16*(6), 2373–2402. https://doi.org/10.5194/tc-16-2373-2022

Webster, M. A., Rigor, I. G., Nghiem, S. V., Kurtz, N. T., Farrell, S. L., Perovich, D. K., & Sturm, M. (2014). Interdecadal changes in snow depth on Arctic sea ice. *Journal of Geophysical Research: Oceans*, *119*(8), 5395–5406. https://doi.org/10.1002/2014JC009985

Willatt, R., Laxon, S., Giles, K., Cullen, R., Haas, C., & Helm, V. (2011). Ku-band radar penetration into snow cover on Arctic sea ice using airborne data. *Annals of Glaciology*, *52*(57), 197–205. https://doi.org/10.3189/172756411795931589